Modeling of electron-cyclotron-resonance-heated plasmas

A. Girard, C. Pernot, and G. Melin
Département de Recherche Fondamentale sur la Matière Condensée, SI2A, CEA Grenoble, 17 rue des Martyrs, 38054 Grenoble Cedex 9, France

C. Lécot
Laboratoire de Mathématiques, Université de Savoie, Campus Scientifique, 73376 Le Bourget-du-Lac Cedex, France
(Received 16 November 1999; revised manuscript received 22 February 2000)

This article describes the behavior of electron-cyclotron-resonance-heated plasmas, with particular attention paid to mirror-confined plasmas, which are of great interest in plasma processing and in highly charged ion production. Using a one-dimensional (in velocity) description of the electron distribution function, we calculate the electron density and confinement time. The theoretical results are compared with experiments, and it is shown that a maximum critical density can be achieved in such plasmas.

PACS number(s): 52.65.Ff, 29.25.Ni, 52.50.Gj, 52.55.Jd

I. INTRODUCTION

Electron-cyclotron-resonance (ECR) heated plasmas are encountered in various fields of research and industry [1]. They can be used for ion implantation, surface treatment, and coating in industry; on the other hand mirror-confined ECR-heated plasmas have proved to be very efficient for the production of multiply charged ions (MCIs). This paper deals mainly with such mirror-confined plasmas, but some of the results can be used for other types of ECR-heated plasmas.

In order to produce MCIs in a plasma some criteria have to be fulfilled: (1) Electrons should reach energies larger than the ionization potential of the desired ion. (2) Ions should stay in the plasma for a time sufficient to reach the desired charge state. This criterion follows from the dominant stripping process in the plasma, which is the step by step ionization of atoms and ions. (3) The neutral pressure should be kept low enough so that charge exchange processes between ions and atoms are negligible. As can be easily understood, these criteria are ideally achieved in a mirror-confined ECR-heated plasma: electrons are pushed toward high energies owing to the ECR heating (ECRH); the confinement time is good because of the mirroring of the particles between the two maxima of the magnetic field; the third criterion is fulfilled when only a small amount of gas is injected into the plasma. Figure 2 of [2] shows the currents of MCIs that can be delivered by the SERSE, source, which is a high performance superconducting ECR ion source (ECRIS).

Figure 1 shows a schematic drawing of an ECRIS: the minimum-**B** structure is achieved with coils (1) and (2) for the mirror field and permanent magnets (3) for the multipole field (usually hexapolar). The electrons interact resonantly with the wave close to the resonance surface (4) which is shaped like an ellipsoid. The high frequency (HF) wave is injected along the magnetic field (the magnetic beach structure) and the whole chamber is biased at typically +20 kV. Ions are then extracted through a grounded extraction electrode.

Some theoretical work has already been done to explain the production of MCIs. The dominant stripping process is step by step electron impact ionization, and among the recombination processes the most important one is charge exchange. But all these studies made the assumption that the electron distribution function (EDF) is Maxwellian [3] or weakly non-Maxwellian [4]. Moreover, the input parameters of these codes, which are usually the electron density and temperature, have to be adjusted to fit the experimental results. These limitations of existing theoretical studies are severe since the electron density and temperature are not input parameters for the experimentalist but rather the results of the source optimization. Therefore these codes may be of limited interest. A new code was recently presented [5] where the input parameters are much closer to reality: the HF power and the gas flux were taken as input parameters and the other parameters of the plasma were calculated. But in this study the EDF was also supposed to be Maxwellian, which led to unphysical values of the plasma potential. A useful and accurate simulation of the plasma requires the calculation of the EDF.

Some articles have dealt with the problem of ECRH in mirror-confined plasmas. The first theoretical studies concerned stochastic (or quasilinear) electron heating, and were published in the early 1970s [6]. A relativistic theory of ECRH was later presented by Bernstein and Baxter [7]. The problem of electron heating in tandem mirrors (which are also open devices, but different from ion sources) was also extensively studied [8]. However, in these devices, the ions are hot, the plasma is not necessarily created only by ECRH, and some approximations can be made concerning the HF and collision diffusion coefficients, which are not relevant to

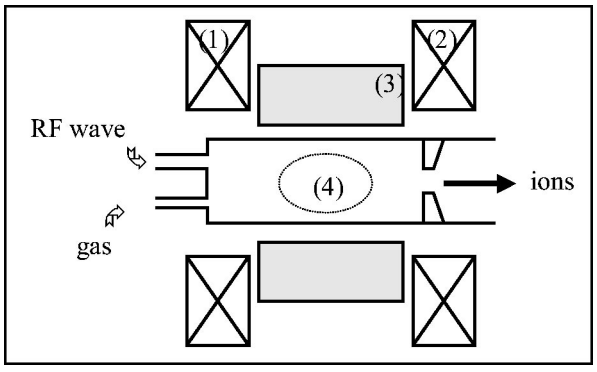

FIG. 1. Principle of an ECRIS.

our devices. The most exhaustive study in the field of ECRH in mirrors was presented by Mauel [9], who calculated the EDF theoretically and applied his calculations to the Constance 2 ECRH experiment. In that experiment it was suggested that the HF itself could enhance the loss of electrons. However, only a transient state was modeled by Mauel and no conclusion was drawn about the steady state that could be reached in ECR-heated plasmas. A few years later [10] the role of HF-induced losses in a micro-unstable ECR heated plasma was discussed. In the present article, however, the plasma will be supposed to be free of any such instability. A recent paper [11] presents new experimental results on an ECRIS and also discusses the influence of the HF-induced transport of electrons on the performance of the ECRIS. The present article explains the results obtained in [11] and gives a theoretical background to the conclusions drawn there from the experimental results. It is also the first step toward a complete self-consistent description of an ECRIS.

This paper is organized as follows. In Sec. II the basic ingredients of the code are presented. The collisional term and the HF term are described and the source term that is necessary to obtain a steady state is also explained. The simplifications made are described and discussed. In Sec. III the numerical results are shown, and the major transport processes are discussed. Comparisons are made with experimental results. In Sec. IV some important conclusions concerning ECR-heated plasmas are drawn.

II. DESCRIPTION OF THE CODE

We assume that the system is uniform in physical space. The time-dependent equation for the EDF is given as

$$\frac{\partial f_e}{\partial t} = C(f_e) + Q(f_e) + S(f_e). \tag{1}$$

Here $C(f_e)$ is the collision term for electrons colliding off other charged species (including electrons themselves), $Q(f_e)$ is the quasilinear heating term which describes ECRH, and $S(f_e)$ describes the ionization processes that generate electrons. Our starting point is the bounce-averaged quasilinear Fokker-Plank equation [12]. We consider the time evolution of the EDF over time intervals much longer than both the cyclotron period $2\pi/\omega_c$ and the bounce period τ_B. The characteristic time scale over which we analyze f_e has therefore the same order of magnitude as the collisional time.

Since we wish to calculate the density that can be reached in an ECR-heated plasma, it is important to take into account the correct collision term. In most of the HF-wave–plasma interactions, the full integro-differential term is not used, since it is possible to assume that the plasma is composed of a bulk of electrons and a HF-wave-generated tail. In our case such an assumption is not possible since the plasma is generated by the HF wave itself and the density that is obtained is not always sufficient to ensure a strong collisional relaxation toward a Maxwellian bulk. Therefore the full collisional term must be used. Then Eq. (1) is a nonlinear, partial, integro-differential equation in four independent variables. We employ the usual spherical polar coordinate system (v,μ,φ) in velocity space, where v is the speed, $\arccos\mu$ is the pitch angle, and φ is the angle about the axial magnetic field. With this coordinate system, we assume that the system is azimuthally symmetric. Hence the resulting distribution function is of the form $f_e(v,\mu,t)$. When no ambipolar field is present, the loss cone angle is given by

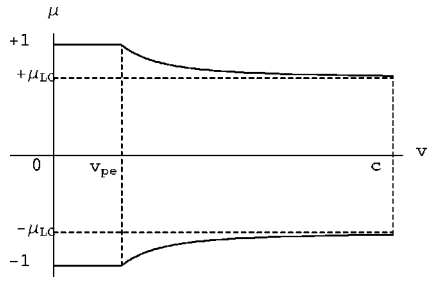

FIG. 2. Velocity domain $\mathcal{U}_e$.

$$\mu_{lc} = \sqrt{1 - 1/R_m}$$

with $R_m = B_{\max}/B_{\min}$ the mirror ratio. When a positive potential V_P is present and reduces the loss of electrons, the boundary of the velocity domain is modified:

$$\mu_{lc}(v) = \left[1 - \frac{1}{R_m}\left(1 - \frac{v_{pe}^2}{v^2}\right)\right]^{1/2} \quad \text{where}$$

$$v_{pe} = \sqrt{2eV_P/m_e}.$$

We assume that electrons in the loss cone are lost immediately. Figure 2 shows the confined domain $\mathcal{U}_e$ (solid lines).

The Fokker-Planck collision term was derived by Rosenbluth, MacDonald, and Judd [13] in the form

$$\begin{aligned} C(f_e) = -\sum_{a=e,i} L^{e/a}\Bigg[& \frac{1}{v^2}\frac{\partial}{\partial v}\left(v^2\frac{\partial^2\psi_a}{\partial v^2}\frac{\partial f_e}{\partial v}\right) + \frac{1}{v^2}\frac{\partial}{\partial v}\left((1-\mu^2)\left(\frac{\partial^2\psi_a}{\partial v\,\partial\mu} - \frac{1}{v}\frac{\partial\psi_a}{\partial\mu}\right)\frac{\partial f_e}{\partial\mu}\right) \\ & + \frac{1}{v^2}\frac{\partial}{\partial\mu}\left((1-\mu^2)\left(\frac{\partial^2\psi_a}{\partial v\,\partial\mu} - \frac{1}{v}\frac{\partial\psi_a}{\partial\mu}\right)\frac{\partial f_e}{\partial v}\right) + \frac{1}{v^2}\frac{\partial}{\partial\mu}\left(\frac{(1-\mu^2)^2}{v^2}\left(\frac{\partial^2\psi_a}{\partial\mu^2} + \frac{v}{1-\mu^2}\frac{\partial\psi_a}{\partial v} - \frac{\mu}{1-\mu^2}\frac{\partial\psi_a}{\partial\mu}\right)\frac{\partial f_e}{\partial\mu}\right)\Bigg] \\ & + \sum_{a=e,i} L^{e/a}\frac{m_e}{m_a}\left[\frac{1}{v^2}\frac{\partial}{\partial v}\left(v^2\frac{\partial\varphi_a}{\partial v}f_e\right) + \frac{1}{v^2}\frac{\partial}{\partial\mu}\left((1-\mu^2)\frac{\partial\varphi_a}{\partial\mu}f_e\right)\right], \end{aligned} \tag{2}$$

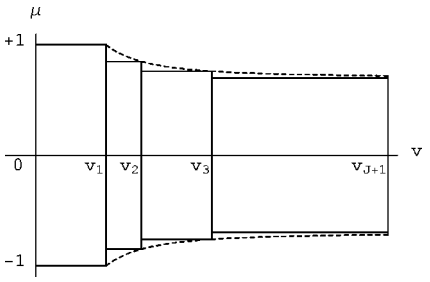

FIG. 3. Discretized velocity domain $\mathcal{U}_e^*$.

where e stands for electrons and i for ions. Here

$$L^{e/a}=\left(\frac{Z_a e^2}{\varepsilon_0 m_e}\right)^2 \lambda$$

with λ the Coulomb logarithm, $Z_a e$ the charge of particles of species a, and φ_a, ψ_a the *Rosenbluth potentials*,

$$\varphi_a(\mathbf{v},t)=-\frac{1}{4\pi}\int_{\mathbf{R}^3}\frac{f_a(\mathbf{v}',t)}{|\mathbf{v}-\mathbf{v}'|}d\mathbf{v}',$$

$$\psi_a(\mathbf{v},t)=-\frac{1}{8\pi}\int_{\mathbf{R}^3}|\mathbf{v}-\mathbf{v}'|f_a(\mathbf{v}',t)d\mathbf{v}',$$

in the form given by Trubnikov [14]. Since the ions are cold and highly collisional, they are assumed to form a fixed Maxwellian background,

$$f_i(v)=\frac{n_i}{(2\pi kT_i/m_i)^{3/2}}e^{-(m_i/2kT_i)v^2}, \tag{3}$$

where n_i is the ion density, m_i is the ion mass, k is the Boltzmann universal constant, and T_i is the ion temperature. The corresponding Rosenbluth potentials are then easily calculated. The velocity domain is discretized as the union $\mathcal{U}_e^*$ of $J+1$ rectangular subdomains $\mathcal{U}_{\text{low}}$ and $\mathcal{U}_j$, $1\leqslant j\leqslant J$, with

$$\mathcal{U}_{\text{low}}=(0,v_{pe})\times(-1,+1),\quad \mathcal{U}_j=(v_j,v_{j+1})\times(-\mu_j,+\mu_j),$$

where $v_1=v_{pe}<\cdots<v_{J+1}=c$, the velocity of light, and $\mu_j=\mu_{lc}(v_{j+1})$, $1\leqslant j<J$, $\mu_J=\mu_{lc}$ (see Fig. 3). The EDF is assumed to be equal to zero outside the discretized velocity domain $\mathcal{U}_e^*$. In addition, we use a numerical model that has proved very useful [12]. The main assumptions of this model are the following. (1) In each subdomain the EDF is approximated by its lowest angular eigenfunction. (2) The Rosenbluth potentials for electrons are isotropic and of the form

$$\varphi_e(v,t)=-\frac{1}{v}\int_0^v \overline{f_e}(w,t)w^2dw-\int_v^{+\infty}\overline{f_e}(w,t)w\,dw, \tag{4}$$

$$\psi_e(v,t)=-\frac{v}{2}\int_0^v \overline{f_e}(w,t)w^2\left(1+\frac{1}{3}\frac{w^2}{v^2}\right)dw-\frac{1}{2}\int_v^{+\infty}\overline{f_e}(w,t)w^3\left(1+\frac{1}{3}\frac{v^2}{w^2}\right)dw, \tag{5}$$

where

$$\overline{f_e}(v,t)=\frac{1}{2}\int_{-1}^{+1}f_e(v,\mu,t)d\mu.$$

On $\mathcal{U}_{\text{low}}$ the EDF is assumed to be isotropic: $f_e(v,\mu,t)=F_e(v,t)$; hence

$$\begin{aligned}C(f_e)=&-L^{e/e}\frac{1}{v^2}\frac{\partial}{\partial v}\left(v^2\frac{\partial^2\psi_e}{\partial v^2}\frac{\partial F_e}{\partial v}\right)\\&-L^{e/i}\frac{1}{v^2}\frac{\partial}{\partial v}\left(v^2\frac{d^2\psi_i}{dv^2}\frac{\partial F_e}{\partial v}\right)\\&+L^{e/e}\frac{1}{v^2}\frac{\partial}{\partial v}\left(v^2\frac{\partial\varphi_e}{\partial v}F_e\right)\\&+L^{e/i}\frac{m_e}{m_i}\frac{1}{v^2}\frac{\partial}{\partial v}\left(v^2\frac{d\varphi_i}{dv}F_e\right).\end{aligned} \tag{6}$$

On $\mathcal{U}_j$ we let $f_e(v,\mu,t)=F_{e,j}(v,t)M_j(\mu)$, where M_j corresponds to the lowest eigenvalue Λ_j of the problem,

$$-\frac{d}{d\mu}\left((1-\mu^2)\frac{dM}{d\mu}\right)(\mu)=\Lambda M(\mu),$$

$$M(-\mu_j)=M(+\mu_j)=0. \tag{7}$$

Then

$$\begin{aligned}C(f_e)=\Bigg[&-L^{e/e}\frac{1}{v^2}\frac{\partial}{\partial v}\left(v^2\frac{\partial^2\psi_e}{\partial v^2}\frac{\partial F_{e,j}}{\partial v}\right)\\&-L^{e/i}\frac{1}{v^2}\frac{\partial}{\partial v}\left(v^2\frac{d^2\psi_i}{dv^2}\frac{\partial F_{e,j}}{\partial v}\right)+L^{e/e}\frac{1}{v^3}\Lambda_j\frac{\partial\psi_e}{\partial v}F_{e,j}\\&+L^{e/i}\frac{1}{v^3}\Lambda_j\frac{d\psi_i}{dv}F_{e,j}+L^{e/e}\frac{1}{v^2}\frac{\partial}{\partial v}\left(v^2\frac{\partial\varphi_e}{\partial v}F_{e,j}\right)\\&+L^{e/i}\frac{m_e}{m_i}\frac{1}{v^2}\frac{\partial}{\partial v}\left(v^2\frac{d\varphi_i}{dv}F_{e,j}\right)\Bigg]M_j.\end{aligned} \tag{8}$$

The term

$$2\pi\int_{\mathcal{U}_e^*}C(f_e)v^2dv\,d\mu$$

is the particle loss term due to collisional pitch-angle scattering.

As to the heating term, we simplify the full quasilinear term [12]. Since this term is not separable in (v,μ), only two terms are retained, so that the diffusion tensor is reduced to a diagonal tensor, and we consider a (mean) velocity diffusion process (heating of the particles due to the HF electric field E) with a pitch-angle scattering process induced by the wave magnetic field. We take the following velocity diffusion coefficient:

$$D_{vv}=\frac{\Delta v^2}{2\Delta t}=D\quad\text{with}\quad D=\pi\left(\frac{eE}{2m_e}\right)^2\frac{d}{L\omega}, \tag{9}$$

where d is the characteristic length for the gradient of the steady magnetic field along the axis, L is the length of the

plasma, and ω is the frequency of the wave. The HF magnetic field contributes to a diffusion coefficient in pitch angle arccos μ:

$$D_{\mu\mu}=\frac{\Delta\mu^2}{2\Delta t}=D\left(\frac{v}{v_\phi}\right)^2, \tag{10}$$

where v_ϕ is the phase velocity of the wave. This term is usually neglected because v_ϕ is considered to be much larger than the velocity of the particles (in many cases the phase velocity is of the order of the velocity of light). But in ECR-heated plasmas the heating process occurs along the whistler mode which has a resonance at $\omega=\omega_c$, the cyclotron frequency. As the wave approaches the resonance zone its phase velocity becomes smaller and smaller. It is therefore necessary to keep the pitch-angle diffusion term in the description of ECRH. The HF magnetic field does not lead to any heating, but it induces pitch-angle scattering which, in a mirror device, can push the electrons into the loss cone, as discussed earlier by Kennel and Engelmann [15]. We therefore take the following quasilinear term:

$$Q(f_e)=\frac{1}{v^2}\frac{\partial}{\partial v}\left(v^2 D_{vv}\frac{\partial f_e}{\partial v}\right)+\frac{1}{v^2}\frac{\partial}{\partial \mu}\left((1-\mu^2)D_{\mu\mu}\frac{\partial f_e}{\partial \mu}\right). \tag{11}$$

The term

$$2\pi\int_{\mathcal{U}_e^*} Q(f_e)v^2 dv\, d\mu$$

is the loss term due to quasilinear pitch-angle scattering. The confinement time is the ratio

$$\tau_e(t)=\frac{n_e(t)}{2\pi\int_{\mathcal{U}_e^*}[C(f_e)+Q(f_e)]v^2 dv\, d\mu}$$

with $n_e(t)$ the electron density.

This modeling of ECRH is, of course, only approximate, since the full quasilinear term is more complicated [12]. In particular, in this model all the electrons are considered to interact with the HF wave, which is true only for the electrons that cross the resonance zone during their bouncing between the mirror throats. Moreover, the strength of the interaction is supposed to be the same for all electrons, which is also a simplification. However, this quasilinear term models the diffusive nature of the heating process in both energy and pitch angle, and it allows us to describe satisfactorily the most salient features of ECRH, as will be shown below. In addition, this term leads to a Fokker-Planck equation that can be solved easily.

Turning to the source term, we consider three possible mechanisms.

(1) The ionization in the volume of the plasma produces electrons as follows:

$$S_{\text{ion}}(v,\mu,t)=2\pi\chi(v)n_i\int_{\mathcal{U}_e^*} f_e(v',\mu',t)\sigma_{0\to i}(v') \times v'^3 dv' d\mu', \tag{12}$$

where $\sigma_{0\to i}$ is the ionization cross section of the atoms and χ is a shape function satisfying

$$4\pi\int_0^{v_{pe}}\chi(v)v^2 dv=1 \quad \text{and} \quad \chi(v)=0 \quad \text{if} \quad v>v_{pe}. \tag{13}$$

In what follows only single ionization of neutrals will be considered.

(2) As they leave the plasma and hit the walls, the ions and electrons may induce secondary electrons. In this process, the material of the wall is of fundamental importance. The corresponding source term may be written

$$S_{\text{wall}}(v,\mu,t)=A\frac{n_e(t)}{\tau_e(t)}\chi(v), \tag{14}$$

where the coefficient A depends on the material.

(3) A third source term can be added to take into account the direct injection of electrons into the plasma through a cathode, or through an auxiliary discharge, which is usually called a *first stage*. We write

$$S_{1\text{st}}(v,\mu,t)=I_e\chi(v). \tag{15}$$

The source term is then defined by

$$S(f_e)=S_{\text{ion}}+S_{\text{wall}}+S_{1\text{st}}.$$

III. RESULTS AND DISCUSSION

We have developed a code applicable to ECR-heated plasmas. We solve the Sturm-Liouville problem (7) by a finite-element method. A finite-difference method is used for discretizing the variable v. The time is discretized by a semi-implicit scheme, i.e., the scheme is implicit but the Rosenbluth potentials are treated explicitly.

Some tests were performed to make sure that the code has a correct behavior. In particular, we verified that the code converges toward a quasi-Maxwellian distribution function when the HF driving term is low. Typically, we used 500 points in μ to solve the Sturm-Liouville problem with sufficient accuracy. For the radial (velocity) problem we used 20 subdomains with 500 points for the domain between 0 and v_1, and 2000 points for the rest of the domain (between v_1 and c). The time step was adjusted between 1 and 100 μs. The code has some input parameters. We consider helium (mass number 4), with the corresponding ionization cross section given in the program, and the mean charge can be varied. In the following we always take $Z_i=1$. The ion temperature is low (less than 1 eV) and therefore has no influence on the ionic Rosenbluth potentials. The HF diffusion coefficient, the mirror ratio, the phase velocity of the wave, the plasma potential, and the neutral density are input parameters of the code. We show the effect of these various input parameters on the plasma performance (electron density and mean energy, confinement time, and absorbed power). Only one parameter is varied at a time.

A. Influence of the mirror ratio

It is well known that the greater the mirror ratio, the higher the confinement, and consequently the higher the den-

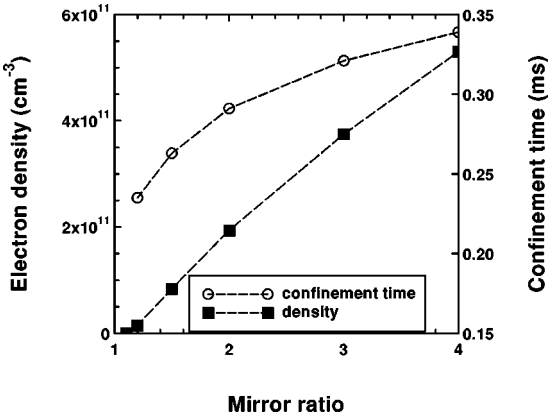

FIG. 4. Electron density and confinement time as a function of the mirror ratio.

sity. Figure 4 shows the increase in density when the mirror ratio is increased, all other parameters being kept constant. This figure explains why a great improvement in performance was obtained when the mirror ratio was increased from 1.3 to 2 in the Caprice source (cf. Fig. 2 of [16]). In our test case, the density is multiplied by a factor of 4 as the mirror ratio is increased from 1.3 to 2. On the same figure one can see that the confinement time also increases as the mirror ratio increases, which is expected, since the mirror ratio is a characteristic of the confining properties of mirror devices. The order of magnitude of the confinement time is compatible with the measurements already presented [11] (this time was sometimes higher, sometimes lower, depending on the characteristics of the discharge), and with the production of high charges. In Fig. 5 the electron mean energy (as the EDF is far from thermodynamic equilibrium it is not possible to use the term ''temperature'') is shown to increase with increasing mirror ratio, which is normal, as the loss term is reduced. Figure 5 also shows the power absorbed (or evacuated) by the electrons, versus the mirror ratio: this power is low at low mirror ratio because the density of the plasma created is low, and it increases at higher mirror ratios as the density and energy increase. It is important to mention here that these results are obtained at the same HF diffusion coefficient (i.e., at the same driving electric field): the same

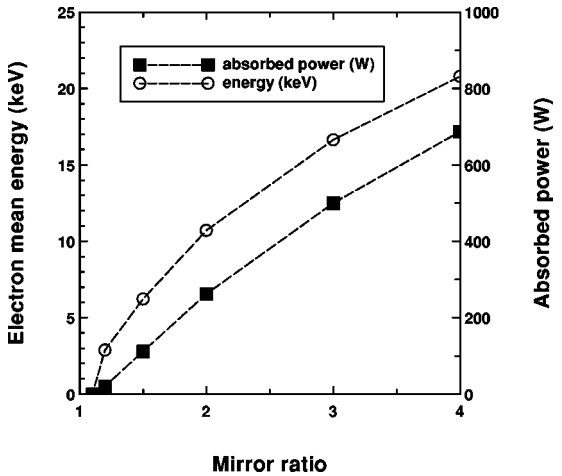

FIG. 5. Electron mean energy and absorbed power as a function of the mirror ratio.

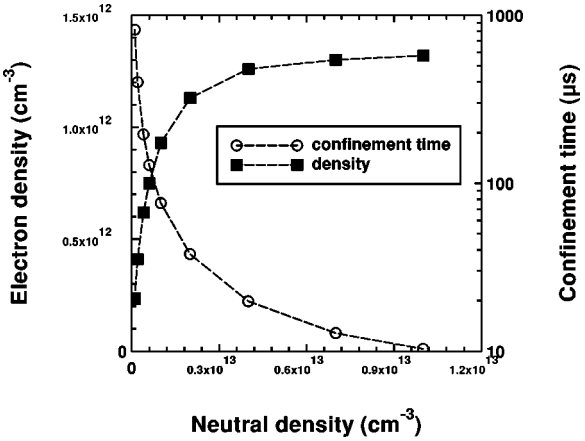

FIG. 6. Electron density and confinement time as a function of the neutral density.

electric field leads to different discharge parameters as the mirror ratio changes. It is of course necessary that the absorbed power be less than the input HF power, which raises the important question of coupling the HF to the plasma. But this point is not addressed here.

B. Influence of the neutral density

Figure 6 shows the evolution of the electron density and confinement time as the neutral density is varied. As usually observed, the electron density is a monotonically increasing function of the neutral gas pressure. However, we see that there is first a rapid increase of the density and then the effect becomes less and less pronounced. Such a behavior was observed in the Quadrumafios source [11]. This effect can be explained as follows: as the neutral density becomes very large the confinement time of the electrons becomes shorter and shorter (see Fig. 6); it would require a huge amount of power to sustain a linear increase of the electron density with the neutral pressure. In the calculation the diffusion coefficient is not sufficient to inject such a high power into the plasma. It is also interesting to see that the higher the neutral density, the lower the confinement time, which explains why it is necessary to work at low neutral pressure to obtain MCIs. Moreover, the value of the confinement time obtained (at low neutral density) is in very good agreement with the experimental results obtained by Perret *et al.* [11], and consistent with the values of the experimental ionic confinement times presented in a recent paper [17]. Figure 7 shows the dependence of the mean energy and of the absorbed power on the neutral pressure: the higher the neutral pressure, the lower the mean energy (as expected). This is a supplementary explanation of the role of neutral pressure in the creation (or destruction) of high charge states: in order to produce high charges it is necessary to have large electron energies to overcome the ionization potentials; highly energetic electrons can be produced only at low pressures, so that high charges are not compatible with high neutral pressures. As a summary, low pressure operation is required to fulfill two major criteria for the production of high charge states: (i) a high confinement time; (ii) high energy electrons.

C. Influence of the phase velocity of the wave

We saw that the magnetic field of the wave plays a role in the loss of electrons. This is clearly shown in Fig. 8: the

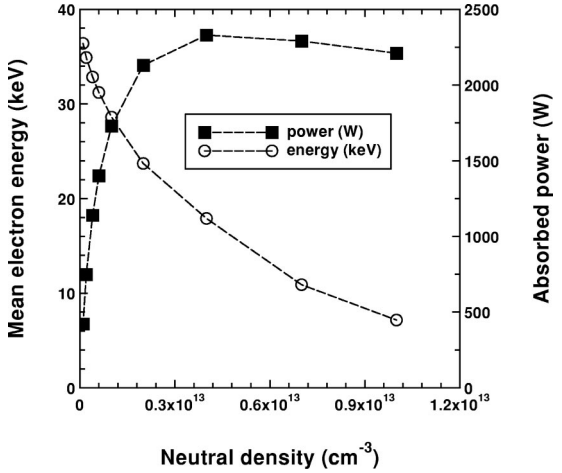

FIG. 7. Electron mean energy and absorbed power as a function of the neutral density.

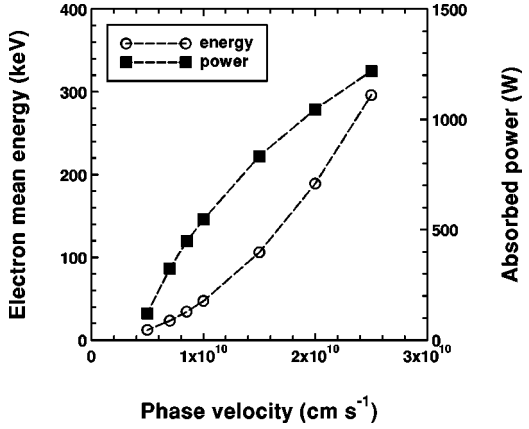

FIG. 9. Electron mean energy and absorbed power as a function of the phase velocity.

higher the phase velocity, the lower the losses (as the calculations are not relativistic, we limit the phase velocity to $2.5c$). Consequently, the electron density is enhanced as the phase velocity increases. The confinement time, also shown in Fig. 8, increases with the phase velocity, since the higher the phase velocity, the lower the HF-induced losses, and consequently the larger the confinement time. Figure 9 shows the electron mean energy versus the phase velocity: it has a quadratic dependence on the phase velocity, since the characteristic energy of the electrons is mv_ϕ^2. In the same figure we see that the absorbed power increases with the phase velocity since both electron density and energy increase.

It is interesting to notice that the mean energy is much higher than the plasma potential (here 30 V). This situation is completely different from what was considered earlier by Pastukhov [18] for mirror-confined fusion plasmas. These high density, lower electron temperature plasmas are usually much closer to thermal equilibrium, and their confinement properties can be described by Pastukhov's model. For ECR-heated plasmas the density that is usually reached (typically $10^{12}\,\mathrm{cm}^{-3}$) is not sufficient for the EDF to relax toward a Maxwellian. This explains why it is necessary to consider the full integro-differential collision term to describe the effect of collisions on the EDF. At low HF power the EDF is close to a Maxwellian, and the collisions are important. At high HF power the HF terms become dominant and the collisions play a role mainly for low energy electrons. The phase velocity of the wave gives an estimate of the maximum mean energy that can be reached in the plasma (see Fig. 9), since electrons below this velocity are mainly heated by the wave, while electrons above this velocity are mainly pitch-angle scattered by the wave magnetic field. We will see below which parameters determine the phase velocity, which is not an input parameter for the experimentalist.

D. Influence of the HF diffusion coefficient

The HF diffusion coefficient is proportional to the square of the electric field, and is consequently related to the HF input power. But the input power is not necessarily equal to the power absorbed by the plasma, which is calculated in the code. Figure 10 shows the evolution of the electron density as D is varied. We see that the density first increases, then saturates, and eventually the density drops. This effect can be explained as follows. The particles are heated with increasing efficiency as the input power is increased, but they are also scattered into the loss cone by the HF input with increasing efficiency. Electrons are heated and lost so rapidly that they are no longer efficient for the ionization, thus limiting the performance of the source. Figure 11 shows the power absorbed (evacuated) by the plasma versus the HF

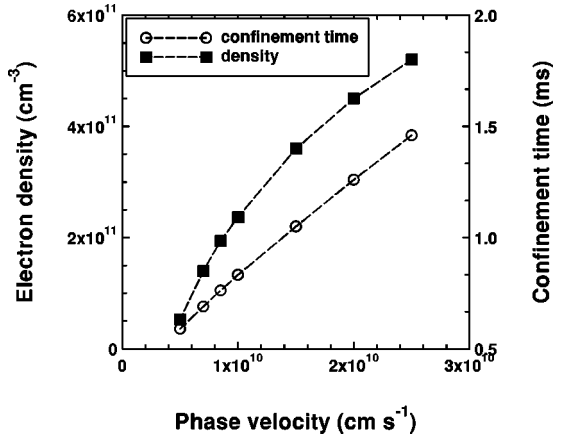

FIG. 8. Electron density and confinement time as a function of the phase velocity.

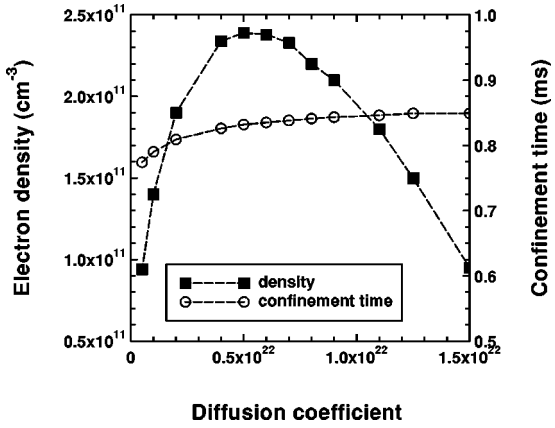

FIG. 10. Electron density and confinement time versus HF diffusion coefficient.

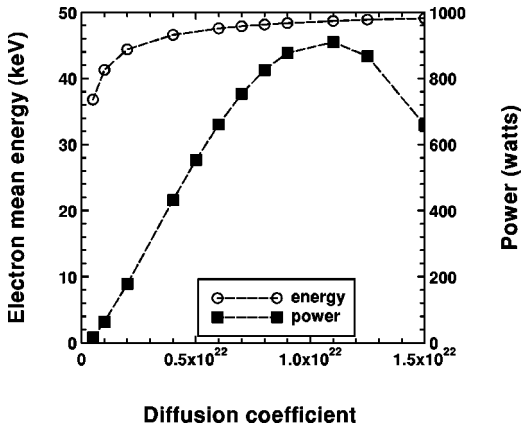

FIG. 11. Electron mean energy and absorbed power versus HF diffusion coefficient.

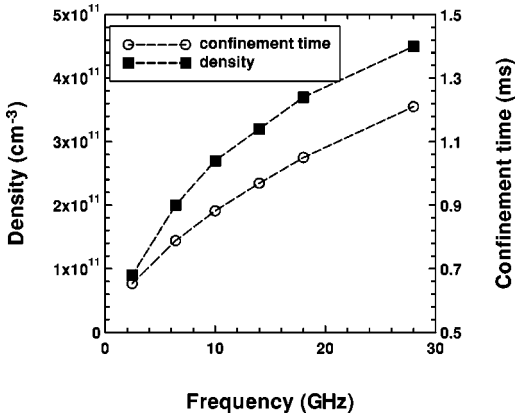

FIG. 12. Electron density and confinement time versus HF frequency.

diffusion coefficient. The maximum of the absorbed power is obtained at a value higher than the maximum of the density, which is quite normal as the power is a second order moment of the EDF, while the density is a zeroth order moment of the EDF. This saturation of the performance is always observed in an ECRIS. However, the decay of the density, as shown in Fig. 10, is rarely observed, since the experimentalists usually stop increasing the (incident) HF power as they see that the performances are no longer improved by additional HF power. But it is often observed that the HF reflected power starts increasing when the performances of the source saturate, which is in agreement with the saturation of the power absorbed by the plasma as shown in Fig. 11. This figure also presents the influence of the HF power on the mean energy of the electron population. It rapidly increases with the HF power and saturates for the same reasons as given above: as the HF power increases, the electrons created by ionization are rapidly heated and lost at high energy. They do not contribute to any increase in density and energy. This rapid saturation of the mean energy of the plasma was observed experimentally first in the Minimafios source [19], and later in the Quadrumafios source [20]. The numerical results are again in very good agreement with the experiments. The confinement time, also shown in Fig. 10, has only a limited dependence on the HF diffusion coefficient, since the range of the mean energy (beyond 20 keV) is such that Coulomb collisions become of limited effect, and the dominant HF losses are characterized by the same phase velocity.

E. Discussion

We have shown that the phase velocity of the wave affects both electron density and mean energy. In order to have both a high density and a high energy plasma, it is therefore necessary to have a high phase velocity. But this is not always possible, and we show in the following how the value of the phase velocity is dependent on plasma parameters. It is well known that the dispersion equation for whistler wave propagation is given, in the cold plasma limit, by

$$\frac{k^2c^2}{\omega^2}=1-\frac{\omega_p^2}{\omega(\omega-\omega_c)}, \tag{16}$$

where k is the modulus of the wave vector and ω_p is the plasma frequency. This formula is valid up to the absorption zone, whose width is given by the Doppler effect:

$$\omega=\omega_c-kv_T, \tag{17}$$

where v_T is the thermal velocity of the electrons. Equation (16) is no longer valid when $|\omega-\omega_c|$ is equal to kv_T, so that an estimate of k is then given by

$$\frac{k^2c^2}{\omega^2}\approx-\frac{\omega_p^2}{\omega k v_T}. \tag{18}$$

Taking the phase velocity $v_\phi=\omega/k$, we obtain

$$v_\phi^3\approx\frac{\omega^2}{\omega_p^2}v_Tc^2=\frac{n_c}{n_e}v_Tc^2, \tag{19}$$

where

$$n_c=\frac{\omega^2 m_e\epsilon_0}{e^2}$$

is the so-called cutoff density, which is proportional to the square of the HF frequency. Equation (19) shows that the larger the density (as compared to the cutoff density), the smaller the phase velocity. But we have shown that the smaller the phase velocity, the smaller the density that can be reached. Therefore, in order to reach a high density, it is necessary to have a large cutoff density (i.e., a large frequency). Equation (19) can be added to the code, so that the phase velocity, which was an input parameter of the code, becomes a function of other plasma quantities. It then becomes possible to plot—all other parameters being kept constant—the plasma density and confinement time versus the frequency of the wave: this is shown in Fig. 12. The electron mean energy and the absorbed power are shown in Fig. 13. These figures show that only high frequencies can produce high plasma densities with high confinement times, which is the condition for the production of high charge states. This explains why the performances of ion sources are enhanced when the frequency is increased (cf. Fig. 3 of [16]). In order to produce MCIs it is necessary to keep the neutral pressure low enough to minimize charge exchange. Therefore the neutral density cannot be arbitrarily increased. As the electron density increases the phase velocity de-

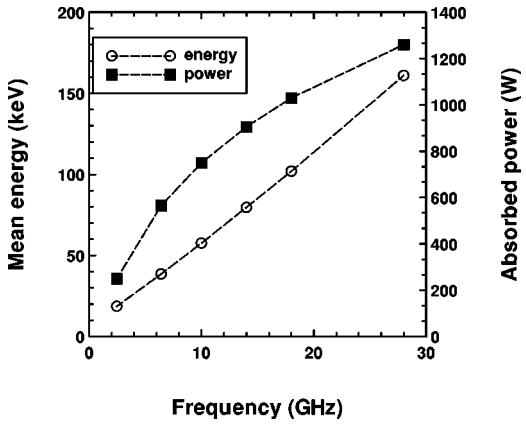

FIG. 13. Electron mean energy and absorbed power versus HF frequency.

creases as shown by Eq. (19). Therefore there is a maximum density compatible with the production of high charge states; the higher the frequency of the wave, the higher this density. This effect has no link, however, with a reflection of the wave at the cutoff density since there is no such cutoff along the whistler branch. Equation (19) can also explain the saturation effect that is encountered in overdense ECR-heated plasmas: at 2.45 GHz the maximum density is typically $10^{12}\,\mathrm{cm}^{-3}$, which is far above the cutoff density (which confirms that there is no cutoff of the HF wave); in these unconfined ECR-heated plasmas the electron temperature is typically 20 eV, which is much lower than in minimum-**B** structures as ECRISs for MCI production; as the electron temperature is low, it is possible to increase the electron density to a value higher than in ECRISs for the same HF frequency.

IV. CONCLUSION

We have developed a model that can reproduce the behavior of ECR-heated plasmas: the influence of the mirror ratio and of the neutral density on the performances are consistent with experiments. The confinement time obtained in the code is in excellent agreement with experiments. The behavior of the mean energy of the electron population is accurately described. As in the experiments, we have found that the electron density and the electron mean energy saturate with the incident HF power. Moreover, we have proved that the phase velocity strongly affects the electron density and therefore the performances of ECRISs: the smaller this velocity, the smaller the density and the smaller the currents. In ECR-heated plasmas it is therefore necessary to increase the frequency in order to enhance the performance. This shows how the performance of the source can be improved: existing ECRISs work at frequencies below 18 GHz; a considerable enhancement will be obtained with 28 GHz gyrotrons and superconducting solenoids.

[1] R. Geller, *Electron Cyclotron Resonance Ion Sources and ECR Plasmas* (Institute of Physics, Bristol, 1996).
[2] P. Ludwig, F. Bourg, P. Briand, A. Girard, G. Melin, D. Guillaume, P. Seyfert, A. La Grassa, G. Ciavola, S. Gammino, M. Castro, F. Chines, and S. Marletta, Rev. Sci. Instrum. **69**, 4082 (1998).
[3] S. Bliman and N. Chan Tung, J. Phys. (France) **42**, 1247 (1982); G. D. Shirkov, Plasma Sources Sci. Technol. **2**, 250 (1993).
[4] H. I. West, LLNL Report No. UCRL-53391, 1982 (unpublished).
[5] A. Girard and G. Melin, Nucl. Instrum. Methods Phys. Res. A **382**, 252 (1996).
[6] F. Jaeger, A. J. Lichtenberg, and M. A. Lieberman, Plasma Phys. **14**, 1073 (1972); M. A. Lieberman and A. J. Lichtenberg, *ibid.* **15**, 125 (1973); A. J. Lichtenberg and G. Melin, Phys. Fluids **16**, 1660 (1973).
[7] I. B. Bernstein and D. C. Baxter, Phys. Fluids **24**, 108 (1981).
[8] M. Porkolab, L. Friedland, and I. B. Bernstein, Nucl. Fusion **21**, 1643 (1981); T. D. Ronglien, Y. Matsuda, B. W. Stallard, and J. J. Steward, Phys. Fluids B **2**, 338 (1990); I. Katanuma, Y. Kiwamoto, K. Ishii, and S. Mioshi, Phys. Fluids **29**, 4138 (1986).
[9] M. E. Mauel, Phys. Fluids **27**, 2899 (1984).
[10] S. A. Hokin, R. S. Post, and D. L. Smatlak, Phys. Fluids B **1**, 862 (1989).
[11] C. Perret, A. Girard, H. Khodja, and G. Melin, Phys. Plasmas **6**, 3408 (1999).
[12] J. Killeen, G. D. Kerbel, M. G. McCoy, and A. A. Mirin, *Computational Methods for Kinetic Models of Magnetically Confined Plasmas* (Springer, New York, 1986).
[13] M. N. Rosenbluth, W. M. MacDonald, and D. L. Judd, Phys. Rev. **107**, 1 (1957).
[14] B. A. Trubnikov, Rev. Plasma Phys. **1**, 105 (1965).
[15] C. F. Kennel and F. Engelmann, Phys. Fluids **9**, 2377 (1966).
[16] D. Hitz, G. Melin, and A. Girard, Rev. Sci. Instrum. **71**, 839 (2000).
[17] G. Douysset, H. Khodja, A. Girard, and J. P. Briand, Phys. Rev. E **61**, 3015 (2000).
[18] V. P. Pastukhov, Nucl. Fusion **14**, 3 (1974).
[19] C. Barué, M. Lamoureux, P. Briand, A. Girard, and G. Melin, J. Appl. Phys. **76**, 2662 (1994).
[20] A. Girard, P. Briand, G. Gaudart, J. P. Klein, F. Bourg, J. Debernardi, J. M. Mathonnet, G. Melin, and Y. Su, Rev. Sci. Instrum. **65**, 1714 (1994).